High-Throughput Phenotyping: Application to Maize Breeding

Ewerton Lélys Resende , Adriano Teodoro Bruzi * , Everton da Silva Cardoso , Vinícius Quintão Quintão Carneiro , Vitorio Antônio Pereira de Souza , Paulo Henrique Frois Correa Barros , Raphael Rodrigues Pereira

Posted Date: 12 December 2023

doi: 10.20944/preprints202312.0815.v1

Keywords: Crop genetics; Biometrics; Data acquisition and assimilation

Article

High-Throughput Phenotyping: Application to Maize Breeding

Ewerton Lélys Resende [1,*], Adriano Teodoro Bruzi [2], Everton da Silva Cardoso [1], Vinícius Quintão Carneiro [1], Vitório Antônio Pereira de Souza [2], Paulo Henrique Frois Correa Barros [2] and Raphael Rodrigues Pereira [2]

[1] Universidade Federal de Lavras, Departamento de Biologia, Lavras, MG, Brazil, elresendeagro@outlook.com (E.R.); cardoso.xs@hotmail.com (E.C.); vinicius.carneiro@ufla.br (V.C.)
[2] Universidade Federal de Lavras, Departamento de Agricultura, Lavras, MG, Brazil, adrianobruzi@ufla.br (A.B.); vitorioapsouza@gmail.com (V.S.); paulo.barros@estudante.ufla.br (P.B); raphael.pereira1@estudante.ufla.br (R.P.)
* Correspondence: adrianobruzi@ufla.br; elresendeagro@outlook.com

Abstract: The objective was to estimate the correlation between VIs and grain yield and identify the optimal timing and VIs for precise corn grain yield estimation. Furthermore, the study aims to employ photographic quantification to measure corn ear traits and establish their correlation with corn grain yield. Ten corn hybrids were evaluated in CRB with three replications at three locations. Vegetation indices and green leaf area were estimated throughout the cycle using an unmanned aerial vehicle (UAV) and subsequently correlated with grain productivity. In addition, photographs were taken of the corn ear to estimate their length, width and total number of kernels and compare these values with manual measurements. The experiments consistently demonstrated significant experimental quality across sites, with accuracy ranging from 79.07% to 95.94%. UAV flights carried out at the beginning of the crop cycle revealed a positive correlation between grain productivity and the evaluated indices (NGRDI, VARI, GLI). Regarding the phenotyping of corn ears, the regression coefficients for width, length and TNG were 0.92, 0.88 and 0.62, respectively, indicating an association with manual measurements. However, stage V5 in the localities of Lavras and Ijaci and stage V8 in the locality of Nazareno showed a positive correlation with productivity. The use of images for ear phenotyping is promising as a method for measuring corn components.

Keywords: crop genetics; biometrics; data acquisition and assimilation

1. Introduction

In plant breeding programs, the demand for field phenotyping has seen a significant increasing, mainly driven by the need to understand genotype-by-environment interactions. Thus, improving traits of interest depends on the ability to quantify phenotypes across genotypes replicated over multiple environments [23]. Traditionally, field phenotypic data have been obtained manually, a labor-intensive and time-consuming process that limits the number of measurable traits. However, the expansion of technologies has enabled cost-effective high-throughput phenotyping (HTP) to automatically acquire multisource crop data, which can greatly reduce the manual labor and time required to obtain crop phenotypic information [13].

With HTP, an understanding of crop development is enhanced, bridging the gaps in the relationship between genotype and phenotype. Numerous phenotyping platforms are available to achieve this goal, with aerial phenotyping in the field being a preferred approach. Aerial phenotyping primarily leverages unmanned aerial vehicles (UAVs) equipped with a variety of sensors, including visible-light (RGB) cameras, infrared thermal imagers, LiDAR, multispectral cameras, and hyperspectral sensors. An essential criterion for these sensors is cost-effectiveness, with RGB cameras being a prime example [31]. For instance [39], employed RGB cameras in predicting rice (Oryza

 doi:10.20944/preprints202312.0815.v1

sativa) yield, and similar cameras have been used to estimate yield and other traits in crops like wheat (Triticum spp.), soybean (Glycine max), maize (Zea mays), barley (Hordeum vulgare), and potatoes (Solanum tuberosum) [3-32-12-16-18].

After acquiring images through these technologies, a range of traits related to growth, development, tolerance, resistance, architecture, physiology, ecology, and yield can be estimated. In particular, many studies have employed digital images to derive vegetation indices (VIs), a powerful tool for assessing green vegetation. [39] demonstrated the effectiveness of color indices, such as the Excess green (ExG) and Visible Atmospherically Resistant Index (VARI) calculated from RGB images, in mapping vegetation fractions and their high correlations with rice grain yield. The normalized green–red difference index (NGRDI) derived from RGB images also exhibited strong correlations with the aboveground biomass of peas and oats, with R^2 values ranging from 0.58 to 0.78 [8].

In the context of corn crops, the correlation between VIs and yield varies based on growth stage and the specific index used, with VARI being one of the top-performing indices. Additionally, canopy cover at 47 and 79 days after sowing has shown a strong correlation with corn yield in some corn populations. showed a correlation to grain yield of 0.76 and 0.77, respectively [4].

In corn breeding programs, beyond field-based plant phenotyping, the accurate and efficient phenotyping of corn ears presents a significant challenge. Traits directly associated with grain yield, such as ear length, width, number of rows, and number of grains per ear, are notoriously labor-intensive to measure, especially when evaluating numerous genotypes in selection processes. Moreover, manual phenotyping is vulnerable to inaccuracies due to differences in evaluator qualifications, calibration issues with the equipment used, and evaluator fatigue, both physical and mental.

In response, ear phenotyping through image analysis has emerged as a valuable solution. It offers a non-destructive, cost-effective, and efficient process, demonstrating a strong correlation with manually obtained data. Several studies have showcased the potential of automated ear phenotyping, enhancing the accuracy and speed of field data processing, and helping breeders pinpoint desirable traits for selecting superior genotypes. This technology is making significant contributions to the extraction of information from cereal crops, including corn [14-22-19-1-20-36-10-35]. While some methods involve rotating mechanisms to capture images of the entire ear surface, increasing both cost and time, others opt for the more straightforward acquisition of a single ear image [35-36].

Therefore, this study endeavors to estimate the correlation between VIs and grain yield and identify the optimal timing and VIs for precise corn grain yield estimation. Furthermore, the study aims to employ photographic quantification to measure corn ear traits and establish their correlation with corn grain yield.

2. Materials and Methods

The experiments were conducted in three distinct environments located in the southern region of the Minas Gerais state. The first was in Lavras, situated at a latitude of 21°14' S, a longitude of 45°00' W, and an altitude of 918 meters. The second was in Ijaci, with a latitude of 21°09' S, a longitude of 44°54' W, and an altitude of 920 meters. The third was in Nazareno, positioned at a latitude of 21°12' S, a longitude of 44°36' W, and an altitude of 1008 meters.

In all these environments, the no-till system was employed. The experimental plots consisted of two rows, each five meters in length, spaced 0.60 meters apart. The experimental design used was randomized complete blocks, with three replications. Sowing took place in the first half of November, followed by thinning. Fertilization, pest management, and weed control were carried out in accordance with the recommended practices for corn crops in the region [27].

The evaluated hybrids were derived from four heterotic groups, selected through the Reciprocal Recurrent Selection (RRS) program at the Federal University of Lavras (UFLA). These populations were labeled as A, B, C, and D. Populations A and B are of conventional nature, while populations C and D incorporate Roundup Ready (RR) and Bacillus thuringiensis (BT) technology.

The experiments were conducted separately for the AB and CDpopulations. Where AB included a total of 10 treatments, six AB hybrids,the original populations A and B, in addition to two

 doi:10.20944/preprints202312.0815.v1

commercial hybrids, DEKALB 230 PRO3 and RB 9077 PRO. The same procedure was applied to the CD populations, featuring identical commercial checks.

Grain yield, an important agronomic trait, was determined from the harvested plots. To ensure consistency, the grain moisture content was standardized to 13%, and the yield was expressed in kilograms per hectare ($kg.ha^{-1}$). Manual evaluations were performed on three ears from each plot, and a millimeter caliper was employed to measure characteristics directly associated with grain yield, including:

Length (L): Measured as the vertical distance from the base to the end of the ear.

Width (W): Determined as the horizontal distance between the rows of grains at the ear's midpoint.

Total number of grains (TNG).

For the purpose of correlation studies, RGB digital images of the ears were captured using a professional-grade camera, specifically the Canon EOS 60D D750, equipped with a 35 mm DX lens featuring a built-in autofocus motor, a 1.8f aperture, and a fixed ISO setting (representing the camera's sensitivity to light) at 1200. These images were saved in "JPG" compression format and utilized the RGB color system, comprising red, green, and blue channels.

To ensure high-quality images, a wooden box was equipped with overhead artificial lighting, and a background was employed to provide adequate contrast with the ears to improve image quality. Subsequently, the ear images were analyzed using the OpenCV and skimage packages within the Python software environment to extract the relevant information.

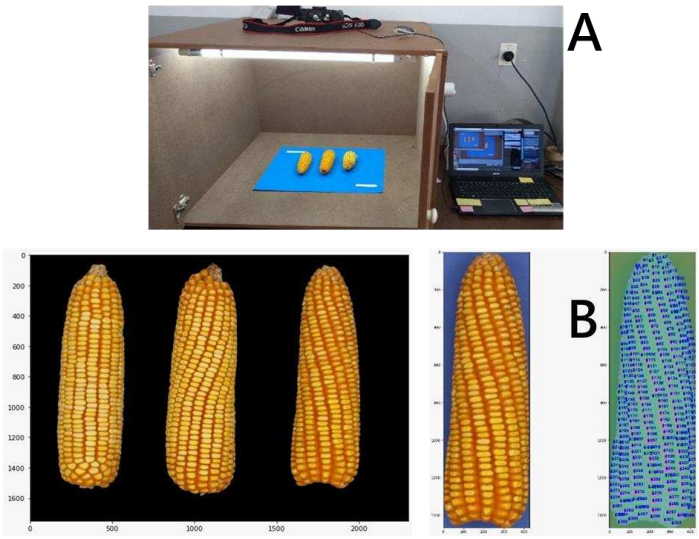

Figure 1. Chamber for image capture (A). Ears without the background and grain count (B).

The UAV utilized in this study was a multirotor (Mavic Pro) equipped with an RGB digital camera. The UAV operations were conducted under favorable weather conditions, characterized by clear skies and low wind speeds, with flights taking place between 10:00 and 14:00 local time. These flights were executed at an altitude of 30 meters. Flight plans were crafted using the Pix4D Capture application program, ensuring 80% longitudinal and 60% lateral overlap for comprehensive image coverage. The subsequent generation of orthomosaics was accomplished using AgiSoft PhotoScan Professional Software. For the analysis of the aerial images and the assessment of crop growth, the R software [25] was employed in conjunction with the FIELDimageR package [20].

In the evaluation and monitoring of crop growth, various vegetation indices were computed. These indices involve algebraic operations on values derived from distinct spectral bands in the visible regions, also referred to as spectral bands. Notably, the indices encompass the normalized green-red difference index (NGRDI), visible atmospherically resistant index (VARI), green leaf index (GLI), and excess green (ExG COLOR INDEX). [33-5-15-21]. Subsequently, these indices enable the

 doi:10.20944/preprints202312.0815.v1

correlation with various crop variables, including biomass, canopy cover, chlorophyll content, and grain yield [29-17].

The flights were performed at different vegetative and reproductive stages to capture the whole crop development (Table 1).

	Flight 1	Flight 2	Flight 3	Flight 4
Ijaci	V5	VT	R3	R5
Lavras	V5	V10	VT	R3
Nazareno	V8	VT	R4	R6

Individual analyses for all traits were carried out using the statistical model as follows:

$$yij = \mu + hi + bj + eij$$

Where:

yij: observed value for the plot that received hybrid i in block j.

μ: constant associated with every observation.

hi: effect of hybrid i.

bj: effect of block j.

eij: error associated with hybrid i in block j.

Furthermore, joint analyses for all traits were performed using the statistical model as follows:

$$yijk = \mu + hi + bj(k) + lk + h*lik + eijk$$

Where:

yijk: observed value for the plot that received hybrid i in block j at location l.

μ: constant associated with every observation.

hi: effect of hybrid i.

bj: effect of block j in location k.

lk: effect of location k.

h*lik: effect of hybrid-by-location interaction.

eijk: error associated with hybrid i in block j at location k.

Experimental precision plays a vital role in ensuring the quality and reliability of trials. Accurate experiments yield more dependable estimates, leading to more precise recommendations. The precision of an experiment is closely tied to its capacity to reproduce results consistently. In this study, the Coefficient of Variation (CV) was employed. The CV considers both the residual variation and the experimental mean. The accuracy of the results depends on the extent of the residual variation, the number of repetitions, and the balance between genetic and residual variations associated with the specific trait being evaluated [28].

To assess experimental precision, the coefficient of variation and accuracy were estimated. Accuracy was determined using the following estimator [28].

$$\hat{rgg} = \sqrt[2]{1 - \left(\frac{1}{F}\right)}$$

where:

F (from Snedecor) is the value of the variance ratio for the effects of treatments (hybrids), associated with the analysis of variance (ANOVA);

The coefficient of variation was estimated using the following estimator:

$$CV = \frac{\sqrt{\sigma_E^2}}{\bar{x}}$$

where:

Preprints (www.preprints.org) | NOT PEER-REVIEWED | Posted: 12 December 2023 doi:10.20944/preprints202312.0815.v1

σ_E^2: residual variation;

x: hybrid means.

Analysis of phenotypic Pearson's correlation between field data (grain yield) and aerial images obtained via UAV was calculated. For digital ear images, the correlation between manual and photographic measurements for width, length, and total number of grains (TNG) traits was performed. To verify the efficiency of phenotyping through digital images and its agreement with manual phenotyping, some reliability measures described in the literature were estimated for these characteristics with the software GENES [2] and R [25].

Reliability measures used:

Coefficient of determination (R^2) of simple linear regression without i intercept (model: Y = βX + e, where Y is the value obtained from the analysis of images, β is the angular coefficient and X the value obtained with manual measurement.

Person (r) correlation (Equation 1), according to the classification proposed by Hopkins (2000).

$$r = \frac{\sum_{i=1}^{n}(X_i - \bar{X}) * (Y_i - \bar{Y})}{\sqrt{\sum_{i=1}^{n}(X_i - \bar{X})^2} * \sqrt{\sum_{i=1}^{n}(Y_i - \bar{Y})^2}}$$

where X_i corresponds to the i-th value obtained with manual measurement, Y_i represents the i-th value observed from the image analysis, X_i is the mean of the values obtained by manual measurement and Y_i is the mean of the values observed from the image analysis.

The Huber M-estimation method (Robust Fit) was used to test the regression. Huber M-estimation finds parameter estimates that minimize the Huber loss function:

$$l(e) = \sum_i p(ei)$$

Where:

$$p\,(e) = \begin{cases} \frac{1}{2}e^2\ if\ |e| < k \\ k|e| - \frac{1}{2}k^2 if\ \ |e| \geq k \end{cases}$$

ei refers to the residuals

The Huber loss function penalizes outliers and increases as a quadratic for small errors and linearly for large errors [6-7].

3. Results and discussion

Individual variance analysis revealed significant differences in grain yield among hybrids in both populations and all three locations. Experimental precision, assessed using the coefficient of variation (CV) and accuracy ($r\hat{g}g^2$), demonstrated high experimental precision with CVs consistently within the low to medium range. Accuracy was also consistently high, ranging from 79.07% to 95.94% across all trials.

Joint variance analysis indicated significant differences between genetic treatments, environments, and hybrid-by-environment interactions for grain yield. Grain yield means varied from 6739 to 12156 kg/ha for the AB population and from 6236 to 12930 kg/ha for the CD population. The Scott–Knott test [30] categorized hybrids into two groups for both populations (Table 2). In the AB trials, RB 9077 and DKB 230 hybrids demonstrated the highest grain yield performance, while the lowest performance was observed in the AB and CD hybrids. For the CD population, RB 9077, DKB 230, HybridCD 1, and Hybrid AB hybrids exhibited the highest grain yield performance.

Preprints (www.preprints.org) | NOT PEER-REVIEWED | Posted: 12 December 2023 doi:10.20944/preprints202312.0815.v1

Table 2. Comparing the grain yield means (kg/ha) of the 10 AB and CD maize hybrids in three different environments using the Scott–Knott test.

Hybrids AB	AB Mean	Hybrids CD	CD Mean
RB 9077	12156a	RB 9077	12930a
DKB 230	10623a	DKB 230	11151a
HybridAB 2	9707b	HybridCD 2	7445b
HybridAB 1	9559b	HybridCD 1	10235a
HybridAB 4	9468b	HybridCD 4	8242b
HybridAB 5	9466b	HybridCD 5	8711b
HybridAB 6	9363b	HybridCD 6	6236b
HybridAB 3	8868b	HybridCD 3	8732b
Hybrid AB	8306b	Hybrid AB	10108a
Hybrid CD	6739b	Hybrid CD	7525b

Means followed by the same letter in the columns belong to the same group by the [30] to the level of 5% probability.

Considering the field phenotyping, the estimation of vegetation indices demonstrated good experimental precision, as indicated by the accuracy and coefficient of variation (data not shown). The precision of these parameters reflects the quality of the trials at the time when the images were captured. Higher precision tends to result in a stronger correlation between yield and the vegetation index, as observed in flights 1, 2, and 3.

Conversely, in flight 4 in the Nazareno location, especially when the trials were assessed at the end of the crop cycles, lower precision was noted. This decrease in precision was attributed to the emergence of weeds after the corn plants began to dry out. Conse

quently, this led to a negative correlation between vegetation indices and yield, with a negative regression slope. A similar observation was made by [37], confirming the impact of weed interference in such situations.

For the joint analysis of all traits, it was found that Location and Flight had statistical significance. Consequently, separate regression analyses were conducted for these traits. Flight 1, during which the plants were in the V5 stage in Lavras and Ijaci and in the V8 stage in Nazareno, exhibited strong R-Square values in relation to grain yield for both populations and all vegetation indices and green leaf areas. In general, the highest R^2 values were observed for the GLI and ExG indices (Table 3). And in the Figure 2 shows the regression slope for each flight in each location.

Table 3. RSquare between four vegetation indices and green leaf area with grain yield (YD) for each of the three locations and each flight.

	Flight 1					Flight 2				
	NGRDI	**VARI**	**GLI**	**ExG**	**Area**	**NGRDI**	**VARI**	**GLI**	**ExG**	**Area**
Lavras	0.07*	0.05	0.09*	0.09*	0.02	0.09*	0.09*	0.07*	0.07*	0.09**
Ijaci	0.03	0.01	0.19**	0.19**	0.01	0.14*	0.14**	0.08*	0.06*	0.15**
Nazareno	0.04	0.03	0.02	0.04*	0.11**	0.07*	0.06*	0.07*	0.07*	0.09**
	Flight 3					**Flight 4**				
	NGRDI	**VARI**	**GLI**	**ExG**	**Area**	**NGRDI**	**VARI**	**GLI**	**ExG**	**Area**
Lavras	0.08**	0.10**	0.03	0.03	0.05	0.003	0.004	0.001	0.001	0.0003
Ijaci	0.08*	0.07*	0.12**	0.13**	0.06	0.02	0.01	0.06*	0.06*	0.00
Nazareno	0.04	0.03	0.03	0.03	0.02	0.12**	0.12**	0.05	0.05	0.001

RSquare coefficient, ** ($p<0.01$), * ($p<0.05$), without asterisk sign nonsignificant according to the Robust Fit test, Huber M-estimation method.

Preprints (www.preprints.org) | NOT PEER-REVIEWED | Posted: 12 December 2023 doi:10.20944/preprints202312.0815.v1

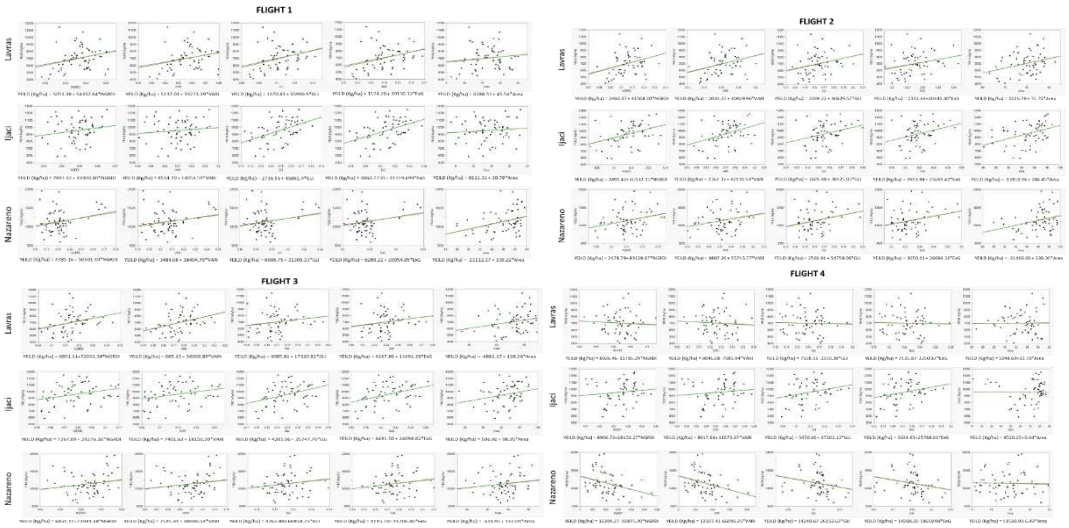

Figure 2. Dispersion graph from the vegetation index and area versus yield for the four Flights and the tree locations and the equation for each the regression graphs.

Recent analyses of durum wheat in Spain have shown RGB picture vegetation indices to consistently outperform multispectral indices such as NDVI in both yield prediction and disease. RGB indices at the canopy level were strongly related to GY and GY losses (R^2 = 0.581; R^2 = 0.536, respectively) associated with disease presence, whereas NDVI was considerably less accurate (R^2 = 0.261; R^2 = 0.277, respectively), especially in the late stage [9]. In the case of corn, the same pattern can be seen. Regarding crop monitoring, RGB vegetation indices derived from canopy pictures were the best parameters for predicting grain yield throughout the nitrogen fertilization treatments (R^2 = 0.721) and outperformed both aerial and ground NDVI (R^2 = 0.689; R^2 = 0.293; R^2 = 0.287, respectively) [9].

Some crops showed a relatively high correlation between the Vegetation Index (VI) and yield; it has been shown that the normalized NGRDI is positively and significantly correlated with the aboveground biomass of peas and oats, with R^2 ranging from 0.58 to 0.78 [8]. However, in the corn crop, the correlation between the VI and yield varied according to the stage and to the index used, where VARI and NGRDI were 0.52 and 0.47, respectively [4]. The same rate was observed in this study. In addition to the VI, the canopy has been reported as a good predictor for corn yield, and canopy cover at 47 and 79 days after sowing showed a correlation to grain yield of 0.76 and 0.77, respectively [4]. According to [34], the precise correlation between yield potential levels in maize with the NDVI index was in the V3 and V8 growth stages, and the highest correlation was in V8; the same was observed in this study.

Corn yield is influenced by multiple factors related to the environment. In addition, maize yield per unit of area is related not only to yield per plant but also to multiple traits, including tolerance to biotic and abiotic stresses, adaptability to the climate and weather, tolerance to planting density, and lodging resistance; these traits create complexities and difficulties for direct correlations between yield and simple traits [38].

Although plant area and VI are associated with yield for maize varieties, yield per plant is largely determined by yield per ear, which is determined by grain number (GN) and grain weight (GW); GN can be decomposed into ear row number (ERN) and GN per row (GNPR). Decomposition of maize yield would facilitate in-depth genetic and molecular studies of maize yield [38].

For corn ear phenotyping, a total of 530 ears displayed substantial phenotypic variation for all descriptors assessed. This diversity was crucial for validating the proposed methodologies as it included various ear patterns. The ear length ranged from 11.8 to 22.6 centimeters, while the width ranged from 3.83 to 6.12 centimeters. The estimate of the regression coefficient (R^2) for width was 0.92 (Figure 3 A), and for length, it was 0.88 (Figure 3 B). These high R^2 values indicated a strong association between the values obtained through manual phenotyping and those extracted from imaging.

Preprints (www.preprints.org) | NOT PEER-REVIEWED | Posted: 12 December 2023 doi:10.20944/preprints202312.0815.v1

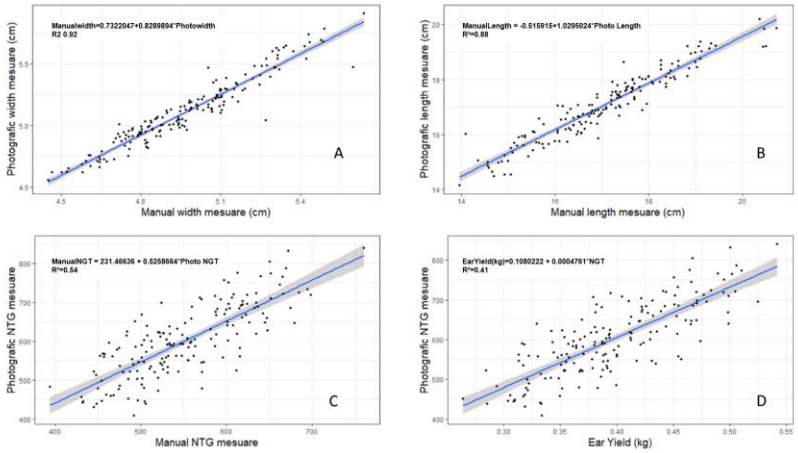

Figure 3. Dispersion graph from manual versus photographic measurements for the traits width (A), length (B), TNG (C), and corn ear yield with photographic TNG measurement (D) and multiple R-squared (R^2).

Width measurements were conducted with a digital pachymeter, ensuring higher precision, while length measurements were taken using a ruler. The validity of these results is further supported by the Pearson's correlation coefficient when calculated separately for different populations and locations (Table 4).

The correlation for TNG ranged from 0.65 in population AB in Ijaci to 0.80 in population CD in Lavras, with an R^2 of 0.62, indicating a strong association with the measurements (Figure 3 C). These graphs confirm the precise estimation of the number of grains, as they demonstrate a strong correlation between TNG and ear yield (Figure 3 D). Generally, manual estimations exhibited lower accuracy for all the assessed traits compared to photographic measurements (Table 4). Phenotyping using images to estimate the number of grains offers significant advantages, including automation, cost-effectiveness, enhanced accuracy in estimations, and reduced time and labor requirements. In contrast, manual measurements are highly subjective and influenced by human factors [14-11-22-19-1-35-36].

Table 4. Accuracy for manual and photographic width, length, TNG and correlation between manual and photographic measurements in the AB and CD populations in Ijaci, Lavras and Nazareno.

	Manual Accuracy			Photographic Accuracy			Correlation		
	Width	**Length**	**TNG**	**Width**	**Length**	**TNG**	**Width**	**Length**	**TNG**
Ijaci AB	68.95	67.94	84.56	77.12	72.85	84.58	0.90**	0.95**	0.65**
Ijaci CD	85.55	74.48	76.00	82.58	73.27	87.86	0.96**	0.98**	0.70**
Lavras AB	65.99	72.54	65.26	81.96	75.20	83.31	0.95**	0.95**	0.79**
Lavras CD	92.39	17.78	78.82	93.66	69.47	83.77	0.98**	0.83**	0.80**
Nazareno AB	57.02	80.58	83.73	71.58	79.97	93.52	0.97**	0.97**	0.75**
Nazareno CD	79.78	82.20	51.23	78.62	80.78	64.96	0.98**	0.97**	0.71**

Pearson's correlation coefficient ** ($p<0.01$), * ($p<0.05$), without asterisk sign nonsignificant correlation according to the T test.

The methodology presented for estimating length and width demonstrated remarkable consistency. Consequently, its adoption in breeding programs has the potential to enhance the efficiency of ear phenotyping while reducing the time required and minimizing human errors in data collection.

These findings align with existing literature, where high concordance indices, approaching unity, were observed in the estimation of leaf area through digital images. Previous studies have similarly concluded that image analysis can effectively replace manual phenotyping by providing more precise measurements of the relevant descriptors [26].

4. Conclusions

The best index related to yield varied due to flight and location. The best time for image collection was between V5 to VT stage. Ear phenotyping based on digital images represents a promising alternative to measure corn yield components. This technique provided greater efficiency and high correlation with manual evaluations.

Author Contributions: Ewerton Lelys Resende: Conceptualization, Formal analysis, Investigation, Methodology, Writing – original draft; Adriano Teodoro Bruzi: Formal analysis, Investigation, Methodology, Supervision, Writing – original draft. Everton da Silva Cardoso: Formal analysis, Investigation, Methodology. Vinícius Quintão Carneiro: Investigation, Methodology. Vitório Antônio Pereira de Souza: Investigation, Writing – original draft. Paulo Henrique Frois Correa Barros: Writing – original draft; Writing - review & editing. Raphael Rodrigues Pereira: Investigation.

Funding: This research received funding from Capes, FAPEMIG and CNPq.

Data Availability Statement: Data are contained within the article.

Acknowledgments: The authors thank the Federal University of Lavras for the structure and the funding bodies.

Conflicts of Interest: The authors declare no conflict of interest.

References

1. CHIPINDU, L., MUPANGWA, W., MTSILIZAH, J., NYAGUMBO, I. & ZAMAN-ALLAH, M. (2020). Maize Kernel Abortion Recognition and Classification Using Binary Classification Machine Learning Algorithms and Deep Convolutional Neural Networks. Ai, v. 1, n. 3, p. 361–375. https://doi.org/10.3390/ai1030024.
2. CRUZ, C. D. GENES (2013). A software package for analysis in experimental statistics and quantitative genetics. Acta Scientiarum. v.35, n.3, p.271-276. https://doi.org/10.4025/actasciagron.v35i3.21251.
3. DI GENNARO, S. F., RIZZA, F., BADECK, F. W., BERTON, A., DELBONO, S., GIOLI, B., TOSCANO, P., ZALDEI, A., & MATESE, A. (2018). UAV-based high-throughput phenotyping to discriminate barley vigour with visible and near-infrared vegetation indices. International Journal of Remote Sensing, v. 39, n. 15–16, p. 5330–5344. https://doi.org/10.1080/01431161.2017.1395974.
4. GARCÍA-MARTÍNEZ, H., FLORES-MAGDALENO, H., ASCENCIO-HERNÁNDEZ, R., KHALIL-GARDEZI, A., TIJERINA-CHÁVEZ, L., MANCILLA-VILLA, O. R. & VÁZQUEZ-PEÑA, M. A. (2020). Corn grain yield estimation from vegetation indices, canopy cover, plant density, and a neural network using multispectral and rgb images acquired with unmanned aerial vehicles. Agriculture, v. 10, n. 7, p. 1–24. https://doi.org/10.3390/agriculture10070277.
5. GITELSON, A. A., KAUFMAN, Y. J., STARK, R. & RUNDQUIST, D. (2002). Novel algorithms for remote estimation of vegetation fraction. Remote Sensing of Environment, v. 80, n. 1, p. 76–87. https://doi.org/10.1016/S0034-4257(01)00289-9.
6. HUBER, P. J. (1973). "Robust Regression: Asymptotics, Conjecture, and Monte Carlo." Annals of Statistics 1:799–821. https://www.jstor.org/stable/2958283
7. HUBER, P. J., & RONCHETTI, E. M. (2009). Robust Statistics. 2nd ed. New York: John Wiley & Sons.
8. JANNOURA, R., BRINKMANN, K., UTEAU, D., BRUNS, C. & GEORG, R. (2014). ScienceDirect Monitoring of crop biomass using true colour aerial photographs taken from a remote controlled hexacopter. Biosystems Engineering, v. 129, p. 341–351. https://doi.org/10.1016/j.biosystemseng.2014.11.007.
9. KEFAUVER, S. C., EL-HADDAD, G., VERGARA-DIAZ, O. & ARAUS, J. L. (2015). RGB picture vegetation indexes for High-Throughput Phenotyping Platforms (HTPPs). Remote Sensing for Agriculture, Ecosystems, and Hydrology XVII, v. 9637, n. October, p. 96370J. https://doi.org/10.1117/12.2195235.
10. KIENBAUM, L., CORREA ABONDANO, M., BLAS, R. & SCHMID, K. (2021). DeepCob: Precise and high-throughput analysis of maize cob geometry using deep learning with an application in genebank phenomics. bioRxiv, p. 2021.03.16.435660.

11. KOMYSHEV, E.; GENAEV, M.; AFONNIKOV, D. (2017). Evaluation of the SeedCounter, a mobile application for grain phenotyping. Frontiers in Plant Science, v. 7, n. January, p. 1–9. https://doi.org/10.3389/fpls.2016.01990.
12. LI, B., XU, X., HAN, J., ZHANG, L., BIAN, C., JIN, L. & LIU, J. (2019). The estimation of crop emergence in potatoes by UAV RGB imagery. Plant Methods, v. 15, n. 1, p. 1–13. https://doi.org/10.1186/s13007-019-0399-7.
13. LI, Y., WEN, W., GUO, X.; YU, Z.; GU, S.; YAN, H. & ZHAO, C. (2021). High-throughput phenotyping analysis of maize at the seedling stage using end-to-end segmentation network. PLoS ONE, v. 16, n. 1 January, p. 1–19. doi: 10.1371/journal.pone.0241528.
14. LIANG, X., WANG, K., HUANG, C., ZHANG, X., YAN, J. & YANG, W. (2016). A high-throughput maize kernel traits scorer based on line-scan imaging. Measurement: Journal of the International Measurement Confederation, v. 90, p. 453–460. https://doi.org/10.1016/j.measurement.2016.05.015.k22
15. LOUHAICHI, M., BORMAN, M. M. & JOHNSON, D. E. (2001). Spatially located platform and aerial photography for documentation of grazing impacts on wheat. Geocarto International, v. 16, n. 1, p. 65–70. https://doi.org/10.1080/10106040108542184.
16. LU, N., ZHOU, J., HAN, Z., LI, D., CAO, Q., YAO, X., TIAN, Y., ZHU, Y., CAO, W. & CHENG, T. (2019). Improved estimation of aboveground biomass in wheat from RGB imagery and point cloud data acquired with a low-cost unmanned aerial vehicle system. Plant Methods, v. 15, n. 1, p. 1–16. https://doi.org/10.1186/s13007-019-0402-3.
17. MAIMAITIJIANG, M., GHULAM, A., PAHEDING, S. & HARTLING, S. (2017). Unmanned aerial system (UAS) - based phenotyping of soybean using multi- sensor data fusion and extreme learning machine. ISPRS Journal of Photogrammetry and Remote Sensing, v. 134, p. 43–58.
18. MAIMAITIJIANG, M.; SAGAN, V.; SIDIKE, P.; HARTLING, S.; ESPOSITO, F.; FRITSCHI, F. B. (2020). Soybean yield prediction from UAV using multimodal data fusion and deep learning. Remote Sensing of Environment, v. 237, February, 111599. https://doi.org/10.1016/j.rse.2019.111599.
19. MAKANZA, R., ZAMAN-ALLAH, M., CAIRNS, J. E., EYRE, J., BURGUEÑO, J., PACHECO, Á., DIEPENBROCK, C., MAGOROKOSHO, C., TAREKEGNE, A., OLSEN, M. & PRASANNA, B. M. (2018). High-throughput method for ear phenotyping and kernel weight estimation in maize using ear digital imaging. Plant Methods, v. 14, n. 1, p. 1–13. https://doi.org/10.1186/s13007-018-0317-4.
20. MATIAS, F. I., CARAZA-HARTER, M. V. & ENDELMAN, J. B. (2020). FIELDimageR : An R package to analyze orthomosaic images from agricultural field trials. The Plant Phenome Journal, n. November 2019, p. 1–6. https://doi.org/0.1002/ppj2.20005.
21. MEYER, G. E. & NETO, J. C. (2008). Verification of color vegetation indices for automated crop imaging applications. Computers and Electronics in Agriculture, v. 63, n. 2, p. 282–293. https://doi.org/10.1016/j.compag.2008.03.009.
22. MILLER, N. D., HAASE, N. J., LEE, J., KAEPPLER, S. M., DE LEON, N. & SPALDING, E. P. (2017). A robust, high-throughput method for computing maize ear, cob, and kernel attributes automatically from images. Plant Journal, v. 89, n. 1, p. 169–178. https://doi.org/10.1111/tpj.13320.
23. MOREIRA, F. F., OLIVEIRA, H. R., VOLENEC, J. J., RAINEY, K. M., & BRITO, L. F. (2020). Integrating High-Throughput Phenotyping and Statistical Genomic Methods to Genetically Improve Longitudinal Traits in Crops. Frontiers in Plant Science, v. 11, n. May, p. 1–18. https://doi.org/10.3389/fpls.2020.00681.
24. PIMENTEL-GOMES, F. P. (2009). Curso de estatística experimental. (15th ed.) Piracicaba. p. 451.
25. R Core Team (2021). R: A language and environment for statistical computing. R Foundation for Statistical Computing, Vienna, Austria. URL https://www.R-project.org/.
26. RAMOS, F. T. , FERREIRA, L. S., PIVETTA, F. & MAIA, J. C. S. (2015). Leaf blade area of different plants estimated by linear and dry matter measures, calibrated with the ImageJ software. V.40, N.8 p. 570-575.
27. RESENDE, E. L., PINHO, R. G. V., SILVA, E. V. V., MASSITELA, J. J., DE SOUZA, V. F. & SOUZA, J. L. D. (2020). Mean components for choosing maize populations to extract inbred lines. Ciencia e Agrotecnologia, v. 44, p. 1–7. https://doi.org/10.1590/1413-7054202044017820.
28. RESENDE, M. D. V. de & DUARTE, J. B. (2007). Precisão E Controle De Qualidade Em Experimentos De Avaliação De Cultivares. Pesquisa Agropecuária Tropical, v. 37, n. 3, p. 182–194. https://doi.org/10.5216/pat.v37i3.1867.
29. SAKAMOTO, T., GITELSON, A. A., NGUY-ROBERTSON, A. L., ARKEBAUER, T. J., WARDLOW, B. D., SUYKER, A. E., VERMA, S. B. & SHIBAYAMA, M. (2012). Agricultural and Forest Meteorology An alternative method using digital cameras for continuous monitoring of crop status. Agricultural and Forest Meteorology, v. 154–155, p. 113–126. https://doi.org/10.1016/j.agrformet.2011.10.014.
30. SCOTT, A.J. & KNOTT, M. (1974). A cluster analysis method for grouping means in the analysis of variance. Biometrics, Washington, v.30, n.3, p.507-512, 1974.
31. SONG, P., WANG, J., GUO, X., YANG, W. & ZHAO, C. (2021) High-throughput phenotyping: Breaking through the bottleneck in future crop breeding. Crop Journal, v. 9, n. 3, p. 633–645. https://doi.org/10.1016/j.cj.2021.03.015.

32. TEWES, A. & SCHELLBERG, J. (2018). Towards remote estimation of radiation use efficiency in maize using UAV-based low-cost camera imagery. Agronomy, v. 8, n. 2, p. 1–15. https://doi.org/10.3390/agronomy8020016.
33. TUCKER, C. J. (1979). Red and photographic infrared linear combinations for monitoring vegetation. Remote Sensing of Environment, v. 8, n. 2, p. 127–150. https://doi.org/10.1016/0034-4257(79)90013-0.
34. VIAN, A. L., BREDEMEIER, C., REGIS, P., DA, F., SANTI, A. L., PAZ, C. & SILVA, D. A. (2018). Critical limits of ndvi for yield potential estimation in maize. (In Portuguese, with English abstract.). Revista Brasileira de Milho e Sorgo, v. 17 n. 1, p. 91-100. https://doi.org/10.18512/1980-6477/rbms.v17n1p91-100.
35. WARMAN, C., SULLIVAN, C. M., PREECE, J.; BUCHANAN, M. E., VEJLUPKOVA, Z., JAISWAL, P. & FOWLER, J. E. A. (2021). Cost-effective maize ear phenotyping platform enables rapid categorization and quantification of kernels. Plant Journal, v. 106, n. 2, p. 566–579. https://doi.org/10.1111/tpj.15166.
36. WU, D., CAI, Z., HAN, J. & QIN, H. (2020). Automatic kernel counting on maize ear using RGB images. Plant Methods, v. 16, n. 1, p. 1–15. https://10.1186/s13007-020-00619-z.
37. YU, N., LI, L., SCHMITZ, N., TIAN, L. F., GREENBERG, J. A. & DIERS, B. W. (2016). Remote Sensing of Environment Development of methods to improve soybean yield estimation and predict plant maturity with an unmanned aerial vehicle based platform. Remote Sensing of Environment, v. 187, p. 91–101. https://10.1016/j.rse.2016.10.005.
38. ZHANG, H., LU, Y., MA, Y., FU, J. & WANG, G. (2021). Genetic and molecular control of grain yield in maize. Molecular Breeding, v. 41, n. 3. https://10.1007/s11032-021-01214-3.
39. ZHOU, X., ZHENG, H. B., XU, X. Q., HE, J. Y., GE, X. K., YAO, X., CHENG, T., ZHU, Y., CAO, W. X. & TIAN, Y. C. (2017). Predicting grain yield in rice using multi-temporal vegetation indices from UAV-based multispectral and digital imagery. ISPRS Journal of Photogrammetry and Remote Sensing, v. 130, p. 246–255. https://10.1016/j.isprsjprs.2017.05.003.